Rheology of Binary Colloidal Structures Assembled via Specific Biological Cross-Linking

Amy L. Hiddessen,[†] David A. Weitz,[§] and Daniel A. Hammer*[,†,‡]

Department of Chemical and Biomolecular Engineering & Laboratory for Research on the Structure of Matter, University of Pennsylvania, Philadelphia, Pennsylvania 19104, Department of Bioengineering, University of Pennsylvania, Philadelphia, Pennsylvania 19104, and Division of Engineering and Applied Sciences/Department of Physics, Harvard University, Cambridge, Massachusetts 02138

Received December 19, 2003. In Final Form: April 30, 2004

The selectivity and range of energies offered by specific biological interactions serve as valuable tools for engineering the assembly of colloidal particles into novel materials. In this investigation, high affinity biological interactions between biotin-coated "A" particles ($R_A = 0.475\ \mu$m) and streptavidin-coated "B" particles ($R_B = 2.75\ \mu$m) drive the self-assembly of a series of binary colloidal structures, from colloidal micelles (a large B particle coated by smaller A particles) to elongated chain microstructures (alternating A and B particles), as the relative number of small (A) to large (B) particles ($2 \le N_A/N_B \le 200$) is decreased at a low total volume fraction ($10^{-4} \le \phi_T \le 10^{-3}$). At a significantly higher total volume fraction ($\phi_T \ge 10^{-1}$) and a low number ratio ($N_A/N_B = 2$), the rheological behavior of volume-filling particle networks connected by streptavidin−biotin bonds is characterized. The apparent viscosity (η) as a function of the shear rate ($\dot{\gamma}$), measured for networks at $\phi_T = 0.1$ and 0.2, exhibits shear-rate-dependent flow behavior, and both the apparent viscosity and the extent of shear thinning increase upon an increase of a factor of 2 in the total volume fraction. Micrographs taken before and after shearing show a structural breakdown of the flocculated binary particle network into smaller flocs, and ultimately a fluidlike suspension, with increasing shear rate. Rheological measurements provide further proof that suspension microstructure is governed by specific biomolecular interactions, as control experiments in which the streptavidin molecules on particles were blocked displayed Newtonian flow behavior. This investigation represents the first attempt at measuring the rheology of colloidal suspensions where assembly is driven by biomolecular cross-linking.

Introduction

Biologically mediated colloidal interactions offer a promising route to the controlled synthesis of new nano- to microscale materials and devices. The availability of complementary biological chemistries with a wide range of affinities provides a tunable approach to assembling colloidal structures. Site-directed assembly of particles into various disordered structures using specific biological receptor−ligand interactions, including streptavidin−biotin,[1,2] antibody−antigen,[3] streptavidin-binding recombinant protein,[4] and selectin−carbohydrate interactions,[5] has been demonstrated in both mono- and bidisperse suspensions. An investigation of nanoparticle aggregation mediated by streptavidin−biotin recognition further showed that aggregation rate and cluster size can be controlled by the concentrations and stoichiometries of these complementary biomolecules.[2] Generally, it is known that, for suspensions of strongly attractive colloids, diffusive collision of the particles leads to irreversible flocculation and fractal structures.[6] Investigations which used high affinity biospecific interactions, such as streptavidin−biotin interactions ($K_a \sim 10^{14}-10^{15}\ M^{-1}$),[7,8] have resulted in strong particle attractions and irreversible aggregation. In the case of streptavidin−biotin cross-linking, irreversible particle binding on experimental time scales can be attributed to the exceptionally slow dissociation rate of the streptavidin−biotin complex ($k_{off} \sim 10^{-6}\ s^{-1}$).[7,9] Lower affinity selectin−carbohydrate interactions ($k_{off} \sim 1\ s^{-1}$)[10−12] have also been exploited to mediate irreversible or reversible colloidal assembly by tailoring the density of biomolecules on particle surfaces. Using high biomolecular surface densities of selectin−carbohydrate chemistry, various kinetically trapped binary colloidal structures were formed by varying the concentration ratio of small to large particles.[5] More recently, particles were made to interact reversibly via selectin−carbohydrate interactions by using significantly lower surface densities.[13] Another study demonstrated the technological utility of colloidal aggregation via protein-based recogni-

* To whom correspondence should be addressed. Current address: Department of Bioengineering, University of Pennsylvania, Suite 120 Hayden Hall, 3320 Smith Walk, Philadelphia, PA 19104-6392. Phone: (215) 573-6761. Fax: (215) 573-2071. Email: hammer@seas.upenn.edu.

[†] Department of Chemical and Biomolecular Engineering & Laboratory for Research on the Structure of Matter, University of Pennsylvania.

[‡] Department of Bioengineering, University of Pennsylvania.

[§] Harvard University.

(1) Connolly, S.; Fitzmaurice, D. *Adv. Mater.* **1999**, *11*, 1202−1205.
(2) Li, M.; Wong, K. K. W.; Mann, S. *Chem. Mater.* **1999**, *11*, 23−26.
(3) Shenton, W.; Davis, S. A.; Mann, S. *Adv. Mater.* **1999**, *11*, 449−452.
(4) Brown, S. *Nano Lett.* **2001**, *1*, 391−394.
(5) Hiddessen, A. L.; Rodgers, S. D.; Weitz, D. A.; Hammer, D. A. *Langmuir* **2000**, *16*, 9744−9753.
(6) Weitz, D. A.; Oliveria, M. *Phys. Rev. Lett.* **1984**, *52*, 1433−1436.
(7) Chilkoti, A.; Stayton, P. S. *J. Am. Chem. Soc.* **1995**, *117*, 10622−10628.
(8) Green, N. M. *Adv. Protein Chem.* **1975**, *29*, 85−133.
(9) Piran, U.; Riordan, W. J. *J. Immunol. Methods* **1990**, *133*, 141−143.
(10) Alon, R.; Hammer, D. A.; Springer, T. A. *Nature* **1996**, *374*, 539−542.
(11) Alon, R.; Chen, S.; Puri, K. D.; Finger, E. B.; Springer, T. A. *J. Cell Biol.* **1997**, *138*, 1169−1180.
(12) Smith, M. J.; Berg, E. L.; Lawrence, M. B. *Biophys. J.* **1999**, *77*, 3371−3383.
(13) Hiddessen, A. L.; Weitz, D. A.; Hammer, D. A. Submitted for publication.

10.1021/la036416i CCC: $27.50
Published on Web 07/10/2004

tion by assembling miniaturized biosensors.[14] However, while previous research has provided valuable insight into the dynamics and utility of colloidal aggregation via specific biological attractions, the material properties (e.g., rheological properties) of the assembled structures are not yet understood.

In contrast, numerous investigations have reported on the microstructure and associated rheological properties of suspensions where assembly was driven by nonspecific particle interactions, including attractive particle interactions of nonbiological origin. Much of this work has focused on the phase behavior[15−18] and rheology[19−23] of monodisperse model hard-sphere suspensions where particles interact only through infinite repulsion on contact. Nonspecific attractions between the particles can be generated by various mechanisms, such as by adding nonadsorbing polymer to induce depletion flocculation,[24,25] or by controlling the solvent quality (e.g., by changes in temperature) to promote the flocculation and gelation of sterically stabilized particles.[26,27] Many studies have probed the rheological properties of suspensions aggregated via nonbiological attractions of varying strengths, including, but not limited to, flocculation due to changes in nonadsorbing polymer concentration,[28,29] electrolyte concentration,[30−34] solvent quality,[35−38] and dispersant concentration (e.g., in carbon black suspensions).[39] In general, and as results from the above studies show, the rheological response, that is, the non-Newtonian behavior, of a suspension can vary widely depending on the nature and strength of the interparticle interactions governing the suspension structure.[40,41]

With the goal of measuring bulk material properties of biocolloidal structures, high affinity streptavidin−biotin surface chemistry has been used to mediate the self-assembly of various disordered binary structures, including extended gel-like materials which have been probed rheologically. Using suspensions of biotin-coated (R_A = 0.475 μm) and streptavidin-coated (R_B = 2.75 μm) polystyrene particles, a series of binary colloidal structures, from colloidal micelles (a large particle coated with smaller particles) to chain microstructures (alternating "A" and "B" particles), was synthesized by decreasing the number ratio of small (A) to large (B) particles ($2 \le N_A/N_B \le 200$) at a low total volume fraction ($10^{-4} \le \phi_T \le 10^{-3}$). At much higher total volume fractions ($\phi_T \ge 10^{-1}$) and a low number ratio ($N_A/N_B = 2$), the rheology of extended, space-filling binary particle networks, connected by streptavidin−biotin bonds, was characterized. Results from steady shear measurements show qualitative similarities to the shear-rate-dependent behavior reported for nonbiological, weakly flocculated suspensions. The measured flow curves (apparent viscosity (η) vs shear rate ($\dot{\gamma}$)) at $\phi_T = 0.1$ and 0.2 show that the viscosity and extent of shear thinning increase upon a 2-fold increase in the total volume fraction. Optical micrographs show that the origin of the shear thinning is the breakdown of the network into flocs which continue to break apart with increasing shear rates. Furthermore, control suspensions of biotin-coated (A) particles and streptavidin-coated (B) particles, where streptavidin sites are blocked with monovalent d-biotin, display Newtonian behavior, providing proof that the microstructures formed in these suspensions, and the rheological properties which describe them, are a result of specific biological cross-linking. These rheological measurements are the first attempts to study the bulk rheological behavior of colloidal suspensions in which structure is mediated by biomolecular interactions (e.g., proteins and oligonucleotides). Future work in this area should generate a more complete description of the rheological properties of these unique materials and facilitate their comparison to other types of aggregating colloidal systems.

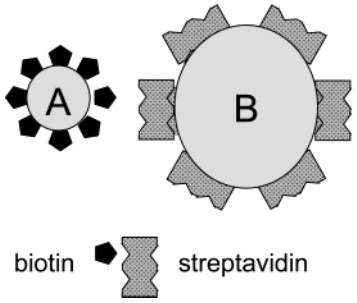

Figure 1. Schematic diagram of the biotin-coated A particles ($R_A = 0.475\ \mu$m) and streptavidin-coated B particles ($R_B = 2.75\ \mu$m) used in this work. The approximate numbers of immobilized biotin (1578 sites/μm^2) and streptavidin (2609 sites/μm^2) surface groups were measured using flow cytometry (Figure 2).

Materials and Methods

Characterization of Streptavidin and Biotin Particles. Two monodisperse populations of polystyrene particles, biotin-modified, $R_A = 0.475\ \mu$m (A particles), and streptavidin-modified, R_B = 2.75 μm (B particles), were purchased from Bangs Laboratories (Fishers, IN) (Figure 1). In preparation for site density determination by flow cytometry analysis, A (biotin-coated) and B (streptavidin-coated) particles were fluorescently labeled with streptavidin−fluorescein (FITC) and biotin−fluorescein (FITC) (Molecular Probes, Eugene, OR), respectively, in phosphate buffered saline solution, pH 7.4, containing 0.01% bovine serum albumin (BSA), 0.01% Tween 80, and 2 mM NaN_3. Soluble labeling concentrations (micrograms per milliliter) for biotin−fluorescein and streptavidin−fluorescein molecules were

(14) Velev, O. D.; Kaler, E. W. *Langmuir* **1999**, *15*, 3693−3698.
(15) Pusey, P. N.; Poon, W. C. K.; Ilett, S. M.; Bartlett, P. *J. Phys.: Condens. Matter* **1994**, *6*, A29−A36.
(16) Pusey, P. N.; van Megen, W. *Phys. Rev. Lett.* **1987**, *59*, 2083−2086.
(17) Pusey, P. N.; van Megen, W. *Nature* **1986**, *320*, 340−342.
(18) van Megen, W.; Underwood, S. M. *J. Phys.: Condens. Matter* **1994**, *6*, A181−A186.
(19) de Kruif, C. G.; van Iersel, E. M. F.; Vrij, A.; Russel, W. B. *J. Chem. Phys.* **1985**, *83*, 4717−4725.
(20) Marshall, L.; Zukoski, C. F. *J. Phys. Chem.* **1990**, *94*, 1164−1171.
(21) van der Werff, J. C.; de Kruif, C. G. *J. Rheol.* **1989**, *33*, 421−454.
(22) Krieger, I. M. *Adv. Colloid Interface Sci.* **1972**, *3*, 111−136.
(23) Mewis, J.; Frith, W. J.; Strivens, T. A.; Russel, W. B. *AIChE J.* **1989**, *35*, 415−422.
(24) Asakura, S.; Oosawa, F. *J. Polym. Sci.* **1958**, *33*, 183−191.
(25) Vrij, A. *Pure Appl. Chem.* **1976**, *48*, 471−483.
(26) Jansen, J. W.; de Kruif, C. G.; Vrij, A. *J. Colloid Interface Sci.* **1986**, *114*, 481−491.
(27) Jansen, J. W.; de Kruif, C. G.; Vrij, A. *J. Colloid Interface Sci.* **1986**, *114*, 471−480.
(28) Patel, P. D.; Russel, W. B. *J. Rheol.* **1987**, *31*, 599−618.
(29) Buscall, R.; McGowan, I. J.; Morton-Jones, A. J. *J. Rheol.* **1993**, *37*, 621−641.
(30) Goodwin, J. W.; Hughes, R. W.; Partridge, S. J.; Zukoski, C. F. *J. Chem. Phys.* **1986**, *85*, 559−566.
(31) Buscall, R.; McGowan, I. J.; Mumme-Young, C. A. *Faraday Discuss. Chem. Soc.* **1990**, *90*, 115−127.
(32) de Rooij, R.; Potanin, A. A.; van den Ende, D.; Mellema, J. *J. Chem. Phys.* **1993**, *99*, 9213−9223.
(33) Folkersma, R.; van Diemen, A. J. G.; Laven, J.; Stein, H. N. *Rheol. Acta* **1999**, *38*, 257−267.
(34) Guo, J. J.; Lewis, J. A. *J. Am. Ceram. Soc.* **2000**, *83*, 266−272.
(35) Woutersen, A. T. J. M.; de Kruif, C. G. *J. Chem. Phys.* **1991**, *94*, 5739−5750.
(36) Grant, M. C.; Russel, W. B. *Phys. Rev. E* **1993**, *47*, 2606−2614.
(37) Rueb, C. J.; Zukoski, C. F. *J. Rheol.* **1997**, *41*, 197−218.
(38) Rueb, C. J.; Zukoski, C. F. *J. Rheol.* **1998**, *42*, 1451−1476.
(39) Trappe, V.; Weitz, D. A. *Phys. Rev. Lett.* **2000**, *85*, 449−452.
(40) Russel, W. B.; Saville, D. A.; Schowalter, W. R. *Colloidal Dispersions*; Cambridge University Press: Cambridge, U.K., 1989.
(41) Larson, R. G. *The Structure and Rheology of Complex Fluids*; Oxford University Press: New York, 1999.

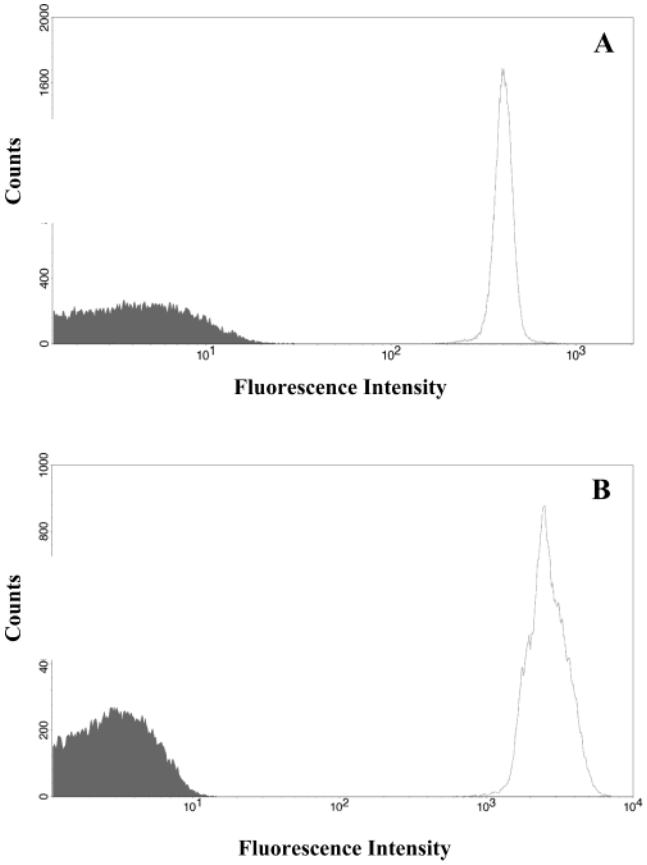

Figure 2. Fluorescence histograms from flow cytometry analysis for (A) biotin-coated A particles and (B) streptavidin-coated B particles. In parts A and B, the peak to the right of the solid reference peak corresponds to A and B particles labeled with saturating concentrations of streptavidin−fluorescein and biotin−fluorescein molecules, respectively. The calculated numbers of biotin sites and streptavidin sites on A and B particles corresponding to the fluorescent intensities of these peaks are 1578 sites/μm^2 and 2609 sites/μm^2, respectively.

varied over several orders of magnitude (0.001−500 μg/mL) to determine the maximum number density of streptavidin or biotin sites, respectively, on the particle surfaces. The fluorescent intensities of negative control (unlabeled A and B particles) and labeled particles (5×10^5 to 1×10^6 particles/mL) were measured using a Becton Dickinson FACS flow cytometer (Becton Dickinson, San Jose, CA), and the resulting fluorescence histograms (Figure 2) were analyzed with Becton Dickinson CellSort software or WinMDI software[42] (Scripps Research Institute FACS Core Facility, La Jolla, CA). Molecular surface site density determination was facilitated by the analysis of fluorescence histograms acquired for fluorescein (FITC) microparticle MESF (molecules of equivalent soluble fluorochrome) standard kits (Quantum 24 FITC low range and Quantum 26 FITC medium range standards, Bangs Laboratories, Fishers, IN). Surface site density estimates for biotin on A particles and streptavidin on B particles were calculated using the standards data and the number of fluorochromes per biotin−FITC or streptavidin−FITC molecule (provided by the manufacturer Molecular Probes).

Preparation of Suspensions for Microscopy. Binary suspensions of biotin-coated, $R_A = 0.475\,\mu$m, particles (A particles) and streptavidin-coated, $R_B = 2.75\,\mu$m, particles (B particles) were made by mixing specific volume fractions of the two individual particle suspensions together with the desired number ratio (N_A/N_B = number of A particles/number of B particles). A schematic representation of the binary particle system studied throughout this work is given in Figure 1. Prior to mixing, A and B particles were washed separately three times and resuspended in phosphate buffered saline (pH 7.4), containing 50 mM NaCl, 1% BSA, and 2 mM NaN_3. Four N_A/N_B ratios were studied ($N_A/N_B = 2$, 10, 100, and 200) at two total number densities. The total volume fractions ($\phi_T = \phi_A + \phi_B$) for the lower total number density experiments were $N_A/N_B = 200$ ($\phi_T = 1.8 \times 10^{-4}$), $N_A/N_B = 100$ ($\phi_T = 2.5 \times 10^{-4}$), $N_A/N_B = 10$ ($\phi_T = 7.0 \times 10^{-4}$), and $N_A/N_B = 2$ ($\phi_T = 9.2 \times 10^{-4}$). For the higher total number density experiments, the total volume fractions were $N_A/N_B = 200$ ($\phi_T = 7.3 \times 10^{-4}$), $N_A/N_B = 100$ ($\phi_T = 1.0 \times 10^{-3}$), $N_A/N_B = 10$ ($\phi_T = 2.8 \times 10^{-3}$), and $N_A/N_B = 2$ ($\phi_T = 3.7 \times 10^{-3}$). For imaging, binary particle solutions were gently loaded into a 30 μL microchamber formed from heat-sealing a glass coverslip to a glass microscope slide with a Parafilm spacer. Inlets were sealed with vacuum grease to prevent sample evaporation. Nonspecific particle−glass interactions were prevented by BSA blocking (1% solution in phosphate buffered saline) of the glass and particle surfaces. Images of the suspensions were acquired using an optical microscope (Nikon Diaphot 200, Tokyo, Japan), equipped with 10−100× (Plan Apo, 1.40 oil 100×) objectives, a black and white Cohu CCD camera (Cohu Inc., San Diego, CA), and a Sony S-VHS recorder (model SVO-9500MD S-VHS, Sony Medical Systems, Montvale, NJ). Snapshot images were acquired during the course of experiments using Imaq Vision software (National Instruments, Austin, TX) on a PC computer (Gateway 2000, Sioux City, SD).

Preparation of Suspensions for Rheology. For rheological measurements, binary suspensions of biotin-coated A particles ($R_A = 0.475\,\mu$m) and streptavidin-coated B particles ($R_B = 2.75\,\mu$m) were prepared by mixing A and B particles at the number ratio $N_A/N_B = 2$ and a total volume fraction of $\phi_T = 0.1$ or 0.2. Prior to mixing, excess BSA and surfactant molecules in particle stock solutions were removed in 10 wash cycles of A and B particles in phosphate buffered saline (pH 7.4, 20 mM NaCl, 0.02% Tween 80), followed by 2 washes and resuspension in phosphate buffered saline (pH 7.4, 20 mM NaCl, 0.02% BSA, 0.02% Tween 80). Control suspensions of B particles only and site-blocked B particles mixed with A particles were prepared by the same procedure. The streptavidin sites on the B particles were blocked with monovalent d-biotin (Sigma Chemicals, St. Louis, MO) prior to the wash cycles. Prior to loading the samples onto the rheometer, all the suspensions were density matched using deuterium oxide (D_2O, 99.9 atom % D, Aldrich Chemicals, Milwaukee, WI). Density matching was tested for each suspension using optical microscopy to verify negligible settling/floating after at least 6 h (typically 12−24 h) and centrifugation to verify negligible settling/floating after spinning for at least 5 min at ≥6000 rpm in a benchtop microtube centrifuge. The final suspensions for all the rheological measurements consisted of the desired volume fractions of particles in H_2O−D_2O phosphate buffered solutions (~50% H_2O/50% D_2O) containing 10 mM NaCl, 0.01% BSA, and 0.01% Tween 80. During the rheology studies, images of the preshear and sheared suspensions were acquired using an optical microscope (Leica inverted microscope, Bannockburn, IL), equipped with 10 to 100× objectives and a Hamamatsu CCD camera (Hamamatsu Corporation, Bridgewater, NJ) and interfaced with PC running SimplePCI imaging software (Compix, Inc., Imaging System, Cranberry Township, PA). To compare the state of the suspension at a series of ascending shear rates ($\dot{\gamma}$'s), 10−15 μL samples were taken directly from the rheometer sample cell and imaged immediately between a glass microslide and a coverglass separated by Parafilm spacers and vacuum grease to prevent evaporation. Since the gel samples were observed to aggregate reversibly after cessation of shear stress, all efforts were made to acquire images in the first few minutes after the sample was extracted from the rheometer. Due to the process of sample transfer from the rheometer to the microscope, these images serve as approximate representations of the state of the suspension after shearing at a given rate.

Rheological Measurements. Steady shear flow curves for all the samples were obtained using a Rheometric Scientific ARES strain-controlled rheometer (Piscataway, NJ) fitted with cone and plate geometry and operating in a torque sensitivity range of 3.9×10^{-7} to 9.8×10^{-4} N·m. Cone and plate geometry was chosen over a Couette cell due to the smaller sample volume, as sample stock was highly valuable. Rheometer calibration was checked with low viscosity standards ($\eta = 0.02$−0.1 Pa·s), and

(42) Trotter, J. *WinMDI*, version 2.8; http://facs.scripps.edu/software.html, 2000.

the results were similar for both geometries. Measurements were made using two sets of stainless steel cone and plate tools with diameters of 25 mm (cone angle of 0.02 rad) and 50 mm (cone angle of 0.04 rad). An aqueous solvent trap and a benchtop humidifier were used to prevent sample evaporation. To maximize reproducibility and minimize potential shear history effects,[37] all the suspensions were presheared for 120 s at a shear rate of $100-300\ s^{-1}$ prior to a premeasurement sample restoration period of 6300 s. Steady shear flow behavior (apparent viscosity (η) vs shear rate ($\dot{\gamma}$)) was measured as a function of ascending shear rate ($\dot{\gamma} = 10^{-2}-10^{3}\ s^{-1}$) at constant temperature (298 K). The results from both the cone and plate tools were combined for multiple runs to establish flow curves.

Results

Effect of the Number Ratio on Heterotypic Assembly. Receptor-mediated assembly of bidisperse suspensions was investigated using A and B particles with high particle surface densities of biotin ($\sim$1578 sites/μm^2) and streptavidin ($\sim$2609 sites/μm^2). At low total volume fractions ($\phi_T = \phi_A + \phi_B = 10^{-4}-10^{-3}$), the effect of the number ratio (N_A/N_B) on suspension microstructure was studied. Four number ratios were examined ($N_A/N_B = 200$, 100, 10, and 2) at two total number densities (see the Materials and Methods section). Although rather dilute total volume fractions were used, interesting structures were able to form because assembly was driven by attractive interactions. For the suspensions at both lower and higher total number densities, an evolving series of binary microstructures was observed upon decreasing the N_A/N_B ratio. As the number ratio of A (biotin-coated) to B (streptavidin-coated) particles decreased, the size and structure of the binary assemblies grew from colloidal micelles (B particles coated by smaller A particles) and small colloidal clusters into colloidal rings and chains of alternating A and B particles (Figure 3). The predominant structure formed at $N_A/N_B = 200$ was the colloidal micelle, where an excess of A particles resulted in the saturation of B particle surfaces by A particles (Figure 3A). The predominant structures formed at $N_A/N_B = 100$ were compact binary colloidal clusters consisting of B particles linked and coated by A particles along with a minority population of colloidal micelles (fewer than at $N_A/N_B = 200$) (Figure 3B). At $N_A/N_B = 10$, the predominant structures were binary rings and chainlike structures (Figure 3C), while, at $N_A/N_B = 2$, the predominant structure was the binary chainlike structure (Figure 3D). Ring and chain structures consist of B particles linked by one or more A particles.

An increase in the total number density did not affect the type of microstructures (colloidal micelles, clusters, rings, or chains) formed at the four number ratios studied but did lead to an increased length scale of the ring and chainlike structures observed at lower number ratios. The structures also evolved more quickly for all number ratios at higher total number densities, as would be expected from mass action. The effect of increased total number density was more dramatic at $N_A/N_B = 10$ and 2, where the self-assembly of more extended networks of binary ring and chainlike structures was observed (Figure 4). At $N_A/N_B = 10$, the increase from a lower to higher total number density led to an increase in the number and diameter of ring structures, and structures became more extended. Binary structures formed in suspensions with $N_A/N_B = 2$ grew to more linearly extended shapes. Regardless of the total number density, the results of these experiments provide evidence that the colloidal structures result from kinetically trapped, diffusion-limited assembly mediated by high affinity streptavidin−biotin interactions. This type of assembly is supported by the fact that, at

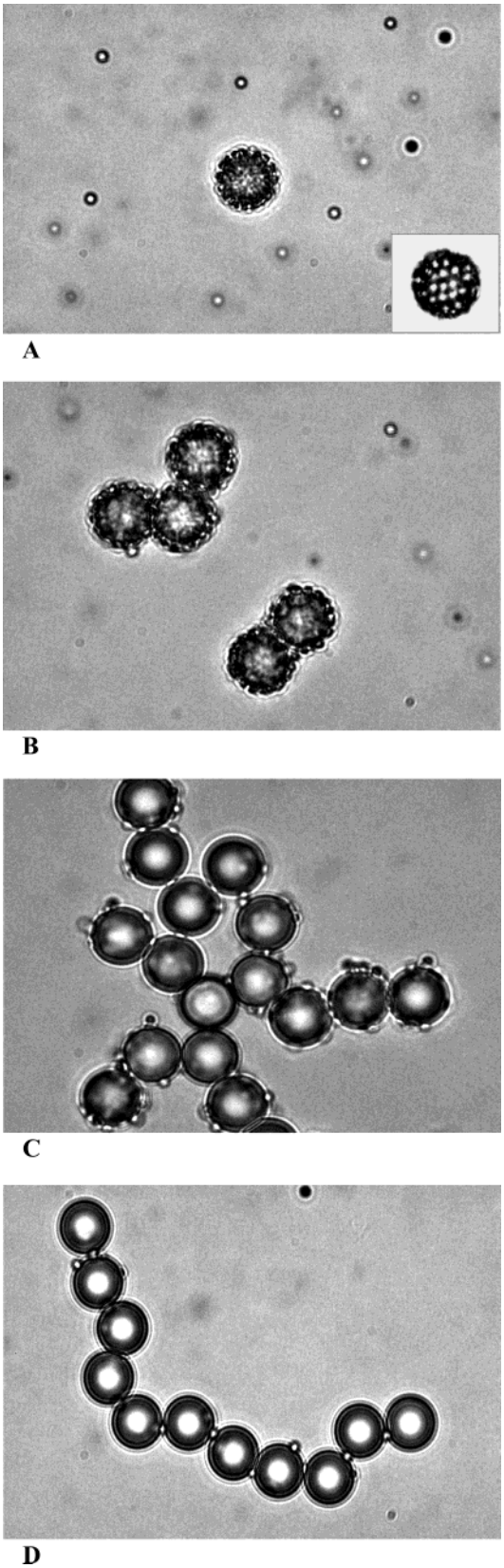

Figure 3. Effect of the particle number ratio (N_A/N_B) on binary colloidal microstructures assembled via specific, streptavidin−biotin interactions. The high magnification optical micrographs (100×) at low total volume fractions ($\phi_T \approx 10^{-4}$) of smaller A (biotin-coated) and larger B (streptavidin-coated) particles for (A) $N_A/N_B = 200$, (B) $N_A/N_B = 100$, (C) $N_A/N_B = 10$, and (D) $N_A/N_B = 2$ show the evolution of suspension microstructures. The inset in part A shows a top view of the three-dimensional structure, where bright circles represent a layer of A particles bound to the surface of a larger B particle.

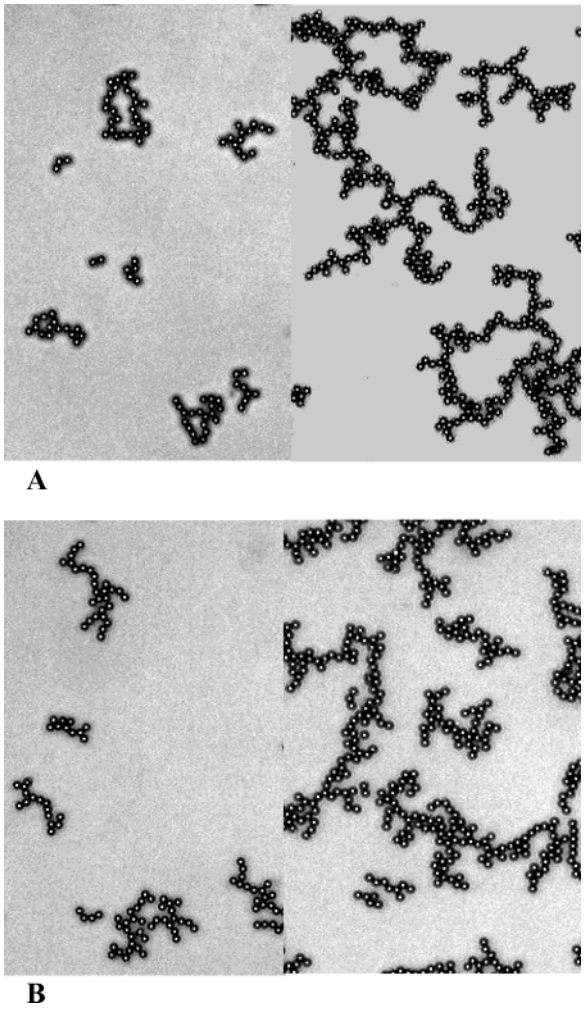

Figure 4. Low magnification optical micrographs (10×) of the binary microstructures formed in the suspensions of A (biotin-coated) and B (streptavidin-coated) particles at (A) $N_A/N_B = 10$ and (B) $N_A/N_B = 2$ at low ($\phi_T \approx 10^{-4}$) and higher ($\phi_T \approx 10^{-3}$) total volume fractions. In parts A and B, the lower total volume fraction micrograph is shown on the left and the higher total volume fraction is shown on the right.

$N_A/N_B = 10$ and 2, disordered macroaggregates did not rearrange or anneal into equilibrium structures during the experimental time frame (1 week). Finally, control experiments in which the streptavidin sites on B particles were blocked with monovalent d-biotin confirmed that the assembly of microstructures is driven by specific biological interactions, as no structures formed (i.e., no aggregation was observed) when these blocked particles were mixed with A (biotin-coated) particles.

Steady Shear Flow Behavior. The steady flow curves (apparent viscosity (η) vs shear rate ($\dot{\gamma}$)) for the binary suspensions ($N_A/N_B = 2$) transformed into gel-like structures by specific binding between streptavidin and biotin were measured at total volume fractions of $\phi_T = 0.1$ and 0.2. A series of control samples prepared at the same total volume fractions were also measured. These include measurements of the suspending fluid without particles (H_2O-D_2O phosphate buffered solution containing 10 mM NaCl, 0.01% BSA, and 0.01% Tween 80) as well as monodisperse suspensions of larger B (streptavidin-coated) particles only and binary suspensions of blocked B particles (the streptavidin surface sites were blocked with monovalent d-biotin) mixed with A (biotin-coated) particles. The flow curves for all the control samples, determined by averaging multiple runs, displayed Newtonian behavior (Figure 5). First, a shear-rate-independent viscosity of $\eta = 9.6 \times 10^{-4}$ Pa·s was measured for the suspending solution, which falls between the viscosities of pure H_2O (η_{H_2O} (25 °C) $= 8.9 \times 10^{-4}$ Pa·s) and D_2O (η_{D_2O} (25 °C) $= 1.1 \times 10^{-3}$ Pa·s). This suspending solution was used for all the particle suspensions. Suspensions of B particles alone at $\phi_T = 0.1$ showed Newtonian behavior, with a constant viscosity of $\eta = 1.45 \times 10^{-3}$ Pa·s, indicating that, in the absence of biotin-coated particles, the suspension remains in a colloidal fluid state. In another control experiment, the streptavidin sites on B particles were blocked with saturating concentrations (0.5 mg/mL) of monovalent d-biotin and subsequently mixed with A (biotin-coated) particles at a total volume fraction of $\phi_T = 0.1$. Again, steady shear measurements revealed shear-rate-independent flow behavior and a constant viscosity of $\eta = 1.41 \times 10^{-3}$ Pa·s. The flow properties of a binary mixture of uncoated polymeric particles (carboxylate-modified lattices, Interfacial Dynamics Co., Portland, OR) having the same diameters of protein-coated particles also displayed Newtonian behavior with a similar viscosity, $\eta = 1.3 \times 10^{-3}$ Pa·s (data not shown).

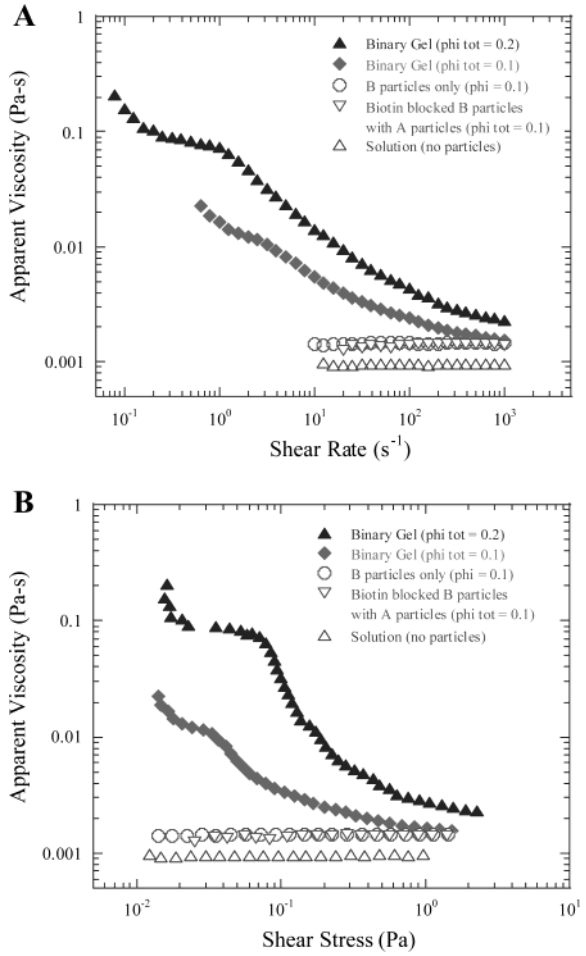

Figure 5. Flow curves for the suspensions cross-linked by streptavidin−biotin chemistry. Apparent viscosity (η) vs (A) shear rate ($\dot{\gamma}$) or (B) shear stress (τ) for the binary suspensions of A (biotin-coated) and B (streptavidin-coated) particles at $N_A/N_B = 2$ and total volume fractions of $\phi_T = 0.1$ (◆) and $\phi_T = 0.2$ (▲), a binary suspension of A particles mixed with blocked B particles (i.e., the streptavidin sites on the B particles were blocked with monovalent d-biotin) (▽) at $\phi_T = 0.1$ ($N_A/N_B = 2$), a monodisperse suspension of B particles only (○) at $\phi_T = 0.1$, and the suspending solution only (no particles) (△).

Density-matched suspensions of streptavidin- and biotin-coated particles self-assembled into volume-filling gel

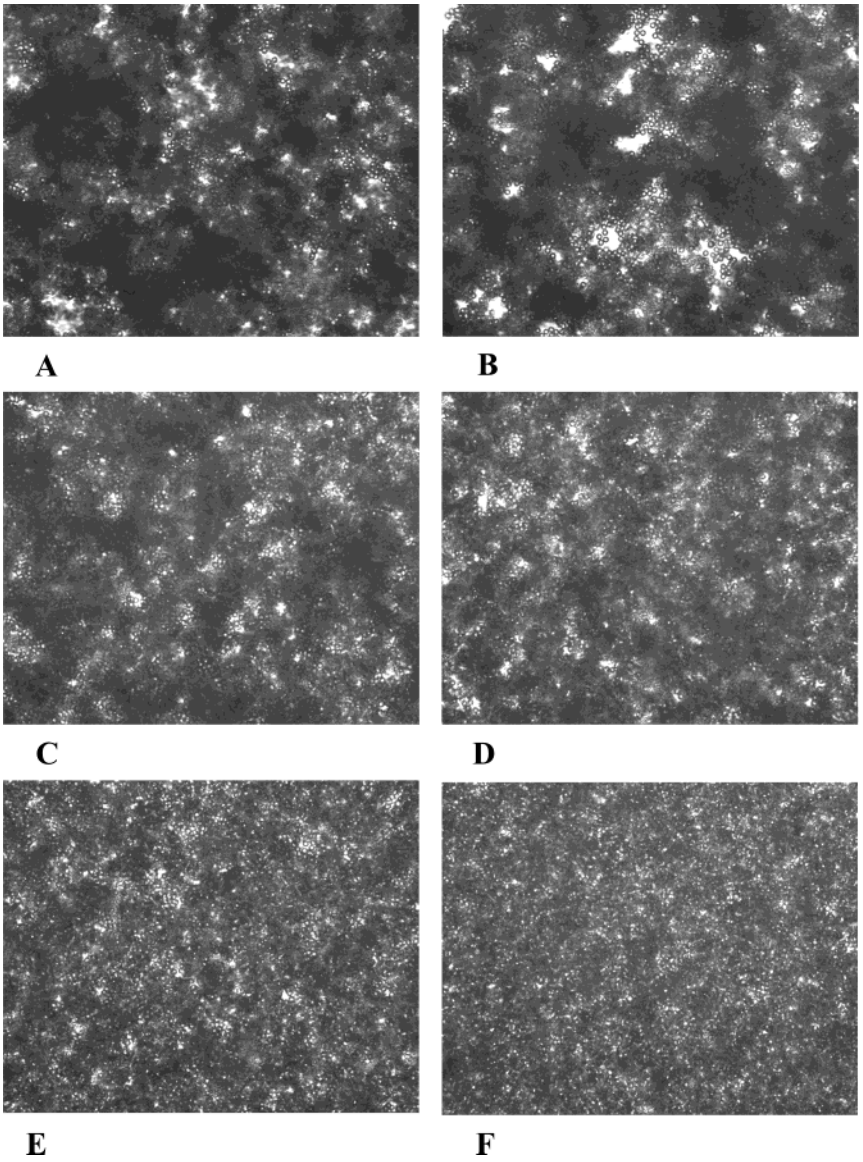

Figure 6. Optical micrographs (20×) of a streptavidin−biotin cross-linked binary gel ($\phi_T = 0.1$) showing the approximate state of the suspension (A) prior to shearing, and after shearing at rates ($\dot{\gamma}$'s) of (B) 6 s^{-1}, (C) 50 s^{-1}, (D) 100 s^{-1}, (E) 300 s^{-1}, and (F) 1000 s^{-1}.

structures and displayed non-Newtonian behavior at total volume fractions of $\phi_T = 0.1$ and 0.2 (Figure 5). The displayed rheological data represent the average of two or more runs (from $\dot{\gamma} = 10^{-2}$ s^{-1} to $\dot{\gamma} = 10^3$ s^{-1}) for each total volume fraction. Gel networks connected by streptavidin−biotin bonds exhibited a shear thinning behavior characteristic of weakly flocculated suspensions, displaying initial viscosities 1−2 orders of magnitude greater than those of the unflocculated control suspensions (Figure 5A). For both total volume fractions, as the shear rate increased, shear thinning led to a reduction of the viscosity to that of the control suspensions. An increase in the total volume fraction from $\phi_T = 0.1$ to $\phi_T = 0.2$ resulted in a greater than 6-fold increase in the initial apparent viscosities and a 4-fold increase in the extent of shear thinning (Figure 5A). At shear rates in the range $\dot{\gamma} \leq$ 1−10 s^{-1}, interesting flow behavior was observed, yet it is not clear whether these features in the flow curves, which suggest a possible yield stress (Figure 5B), represent true behavior or measurement error, such as error due to wall slip effects. Since measurements often fell outside the reliable torque range of the rheometer for shear rates ≤ 1 s^{-1}, additional measurements are needed to draw a firm conclusion on the flow behavior observed at low shear rates.

The physical origin of shear thinning is apparent in a set of micrographs for a binary gel ($\phi_T = 0.1$) that was subjected to a series of increasing shear rates (Figure 6). Initially, the three-dimensional gel is composed of dense flocculated regions connected by thick particle chains, resulting in a space-filling network prior to shearing. After shearing at $\dot{\gamma} = 6$ s^{-1}, the rupture of connective chains commences, and large, dense flocs begin to break away from the network. An increase of 1 order of magnitude in the shear rate leads to more dramatic structural breakdown. At $\dot{\gamma} = 50$ s^{-1}, connective chains have ruptured and the suspension is composed of medium-sized flocs and small clusters of particles which were once part of the network. Particle flocs continue to break apart into smaller units as the shear rate increases over 2 more orders of magnitude until the network is fully destroyed. At the highest shear rates, the suspension breaks down from a mix of small binary clusters and singlets ($\dot{\gamma} = 300$ s^{-1}) to predominantly particle doublets (A−B) and singlets ($\dot{\gamma} =$

1000 s^{-1}). The shear thinning depicted in the flow curves for binary gels (for $\dot{\gamma} \geq 6$ s^{-1}) (Figure 5A) therefore corresponds to a rupturing of the network into discrete flocs that continue breaking down with increasing shear rate. The corresponding reduction of the apparent viscosity toward that of the unflocculated control suspensions provides additional evidence for the structural dissolution of the gel network into a binary fluidlike suspension.

Discussion

High affinity streptavidin−biotin surface chemistry was used to mediate self-assembly of bidisperse suspensions into various disordered structures, from colloidal micelles (a large particle coated with smaller particles) to chain microstructures (alternating A and B particles), by decreasing the number ratio of small (A) to large (B) particles ($2 \leq N_A/N_B \leq 200$) at a low total volume fraction ($10^{-4} \leq \phi_T \leq 10^{-3}$). Using significantly higher total volume fractions ($\phi_T \geq 10^{-1}$) at the lowest number ratio, extended, space-filling binary gel structures were formed in order to study the rheological properties of biologically cross-linked colloidal suspensions. Steady shear rate measurements show these materials exhibit a non-Newtonian, shear thinning flow behavior associated with the breakdown of the gel network into flocs which continue to decrease in size with increasing shear rate.

The number ratio plays a determining role in the types of structures formed, as evidenced by the evolution of colloidal micelles into binary chain structures with decreasing number ratio. An increase in the total number density at number ratios of $N_A/N_B = 10$ and 2 caused the structures to grow into extended networks of rings and chains. Regardless of the total number density, the particle number ratio dictated the number of heterotypic interparticle linkages (B−A−B) that formed. At the two higher number ratios (200 and 100), the saturation of B particle surfaces by smaller A particles prevented B particles from forming heterotypic linkages, thereby limiting the size and shape of the assembled structures. As the number ratio decreased from $N_A/N_B = 100$ to $N_A/N_B = 10$ and 2, B particle surfaces no longer became saturated with A particles; consequently, a greater number of heterotypic linkages formed, and the suspension structure evolved from small clusters to ring and chainlike structures. At $N_A/N_B = 10$, there were often several adherent A particles available at various locations on the larger B particles. This distribution of A particles on B surfaces increased the tendency for multidirectional heterotypic linkages. By contrast, at $N_A/N_B = 2$, there were rarely more than one or two A particles bound to a single B particle. The lack of well-distributed adherent A particles favored more linear growth. Hence, a transition from a network of binary rings and chains at $N_A/N_B = 10$ to elongated, increasingly linear chains at $N_A/N_B = 2$ was observed. The results of these experiments agree very well with a similar study performed with low affinity biological interactions,[5] suggesting that, at high surface densities of biomolecules, where particles are cross-linked by many bonds, kinetically trapped structures form regardless of biological affinity.

At much higher total volume fractions ($\phi_T \geq 10^{-1}$) and a low number ratio ($N_A/N_B = 2$), the rheology of space-filling binary particle networks, connected by streptavidin−biotin bonds, was measured (Figure 5). The steady flow curves (apparent viscosity (η) vs shear rate ($\dot{\gamma}$)) measured at total volume fractions of $\phi_T = 0.1$ and 0.2 revealed a non-Newtonian, shear thinning flow behavior, showing qualitative similarities to the flow behavior observed for steady shear measurements of monodisperse suspensions aggregating via nonspecific attractions.[32,33] The assembly and shear-rate-dependent flow behavior of these gel structures are a result of specific streptavidin−biotin cross-linking, as the flow curves for the control suspensions of A particles and site-blocked B particles displayed Newtonian behavior. Depending on the nature and strength of the particle attraction and the particle concentration, previous research has shown that a Newtonian low shear viscosity plateau or yield stress can be observed prior to shear thinning in flocculating systems.[28,29,38] For example, Buscall et al.[29] measured the steady shear response of nonaqueous suspensions weakly flocculated by depletion effects at a volume fraction of 0.4, finding low shear Newtonian plateau viscosities that increased exponentially with the strength of the interparticle attraction. Separate measurements by Patel et al.[28] of aqueous suspensions flocculated by the addition of nonadsorbing polymer at volume fractions of 0.2 and 0.3 showed apparent yield stresses that increased with volume fraction. In this study, interesting flow behavior, with features suggesting a possible yield stress, was observed prior to the onset of shear thinning; however, it is not yet clear if this is the true behavior. Further measurements are necessary before a firm conclusion can be drawn from the data at the lowest shear rates ($\dot{\gamma} < 1$ s^{-1}). Previous investigations on the steady shear behavior of monodisperse polystyrene dispersions ($0.011 \leq \phi \leq 0.322$) flocculated by electrolyte additions found that viscosity measurements were unreliable at low shear rates ($\dot{\gamma} < 1$ s^{-1}) for $\phi > 0.1$.[32,33] As noted by these authors and as described through systematic investigations conducted by others,[29,43] measurements of the low shear rate behavior for some flocculated colloidal suspensions can be affected by wall slip effects. To further elucidate the steady shear rheology of biospecifically aggregated suspensions, additional tests (e.g., creep measurements) could be performed to probe low shear behavior further. Additional measurements could also facilitate comparison to other flocculated systems, including a model adhesive hard-sphere system for which shear thinning but no yield stress was detected as interparticle attraction was increased at a volume fraction of 0.367.[35]

Optical micrographs of a streptavidin−biotin cross-linked gel at $\phi_T = 0.1$ before and after shearing provide a physical explanation for the measured rheology (Figure 6). The images suggest that the origin of shear thinning is the breakdown of the network into flocs which continue to break apart as the shear rate increases. Prior to shearing, a micrograph of the gelled suspension shows dense flocculated regions connected by thick particle chains. After shearing at a low shear rate, these thick connective chains have thinned or ruptured under imposed shear forces, causing the network to break into large flocs. Micrographs at increasing shear rates reveal that these flocs continue to break down into smaller flocs and binary clusters. Ultimately, at the highest measured shear rate, the network has been destroyed to a fluidlike state, with an apparent viscosity approaching that of the unflocculated control suspensions (Figure 5). A previous study used cryo-SEM to visualize the effect of shear on the structure of flocculated iron oxide suspensions at particle volume fractions of 0.01, 0.033, and 0.094 and reported similar shear-induced elongation and breakup of flocs into smaller units.[44] The study imaged sheared suspensions in the Couette flow cell after a constant applied stress of

(43) Russel, W. B.; Grant, M. C. *Colloids Surf., A* **2000**, *161*, 271−282.

(44) Navarrete, R. C.; Scriven, L. E.; Macosko, C. W. *J. Colloid Interface Sci.* **1996**, *180*, 200−211.

50 Pa (which was well above the observed shear yield stress for these suspensions); however, qualitative agreement with observations reported by the study suggests a possible mechanism for the shear-induced network erosion seen in the series of optical micrographs here: imposed shear forces cause elongation and rupture of the particle network into flocs which gradually decrease in size upon further elongation and rupture at increasing shear rates.

The results of this work contribute to the growing literature on streptavidin−biotin-mediated colloidal assembly and biologically mediated colloidal assembly in general. Earlier studies demonstrated the utility of streptavidin−biotin interactions for site-directed aggregation of both nanoparticles and vesicles, showing aggregate growth rate, shape, and size can be controlled by the ratio of complementary binding sites on colloidal surfaces (biotin) to multivalent cross-linkers (streptavidin) in solution.[2,45] Here, the morphology, size, and growth rate of binary microstructures are controlled by varying the relative and total volume fractions of streptavidin- and biotin-coated particles in bidisperse suspensions. Aside from directing colloidal assembly, high affinity streptavidin−biotin particle interactions have also found uses in mechanical studies of colloidal suspensions. Optical trapping techniques used to study the micromechanical properties of dipolar particle chains in magnetorheological suspensions were facilitated by the use of streptavidin−biotin interactions.[46] In this case, streptavidin-coated particles tethered to the ends of biotinylated, field-induced chains of magnetic particles were manipulated with optical traps to apply forces to the chains. To begin to understand the flow behavior of biologically driven colloidal assemblies under imposed shear forces, this work studied the steady shear rheology of binary suspensions cross-linked into gel-like networks through specific streptavidin−biotin interactions. The non-Newtonian, shear thinning flow behavior of these structures showed a dramatic increase in the low shear viscosity compared to the cases of the control suspensions where specific cross-linking was blocked and Newtonian behavior was measured. These rheological measurements represent the first attempts to study the bulk rheological behavior of colloidal suspensions in which structure is mediated by attractive, biomolecular interactions (e.g., proteins and oligonucleotides). Future measurements on biocolloidal gels should develop a more complete understanding of their rheological properties and facilitate comparison of these properties to those of other aggregating colloidal systems, and perhaps even to those of biopolymer networks.[47] For example, measurements of different biological chemistries over a range of volume fractions could elucidate the rheological response of biocolloid systems as a function of the strength of the specific particle attraction and volume fraction, facilitating comparisons with scaling relationships [39] and theoretical predictions[35,48] developed for suspensions flocculated by nonspecific attractions. Studies on aggregation in flow are not limited to particle systems. For instance, videomicroscopy has been used to investigate the shear rate dependence of the formation and break up of neutrophil aggregates in Couette flow.[49] Further studies of the effects of shear on colloidal particles cross-linked by biomolecular interactions could also contribute to the understanding of aggregation dynamics for cellular networks in which noncovalent, receptor−ligand interactions play a governing role.

Acknowledgment. The authors gratefully acknowledge financial support for this work from NASA (NAG3-211) and NSF MRSEC (DMR00-79909). A.L.H. gratefully acknowledges fellowship support from the NASA Graduate Student Researchers Program and wishes to thank Professor David A. Weitz and all members of the Weitz laboratory at Harvard University for graciously sharing their rheology facility and lab space. The invaluable advice, assistance, and hospitality provided by Dr. You-Yeon Won, Dr. Eric Dufresne, and Dr. Vikram Prasad during these rheology studies is deeply appreciated. A.L.H. is also deeply grateful for invaluable discussions with Professor Paul A. Janmey and Dr. Valeria T. Milam of the University of Pennsylvania.

LA036416I

(45) Kisak, E. T.; Kennedy, M. T.; Trommeshauser, D.; Zasadzinski, J. A. *Langmuir* **2000**, *16*, 2825−2831.
(46) Furst, E. M.; Gast, A. P. *Phys. Rev. Lett.* **1999**, *82*, 4130−4133.
(47) MacKintosh, F. C.; Kas, J.; Janmey, P. A. *Phys. Rev. Lett.* **1995**, *75*, 4425−4428.
(48) Potanin, A. A.; de Rooij, R.; van den Ende, D.; Mellema, J. *J. Chem. Phys.* **1995**, *102*, 5845−5853.
(49) Goldsmith, H. L.; Quinn, T. A.; Drury, G.; Spanos, C.; McIntosh, F. A.; Simon, S. I. *Biophys. J.* **2001**, *81*, 2020−2034.